# Binding of Pyrimidine Model Dimers to the Photolyase Enzyme: A Molecular Dynamics Study

**Jutta Hahn,[†] Maria-Elisabeth Michel-Beyerle, and Notker Rösch***

*Institut für Physikalische und Theoretische Chemie, Technische Universität München, D-85747 Garching, Germany*

*Received: October 27, 1998; In Final Form: January 6, 1999*

Molecular dynamics simulations have been carried out to study structural aspects of the photo repair mechanism of DNA photolyase. In particular, we investigated the docking and binding of bare and dressed model pyrimidine dimers, U⟨⟩T and dU⟨p⟩dT, respectively, in the enzyme pocket. These dimers, which split after photoinduced electron transfer, are essentially inflexible in the gas phase, in water, and inside the enzyme pocket. Details of the dimer docking and the binding inside the pocket are presented and the influence of the desoxyribose and phosphate link on the dimer docking are discussed. The minimum van der Waals distances for the electron transfer between the electron donor $FADH^-$ and the accepting dimers are found to be about 5 Å for U⟨⟩T and about 9 Å for dU⟨p⟩dT. Analysis of the structure of the dimer models and their orientation in the enzyme pocket as well as the orientation of the $FADH^-$ donor suggests that indirect electron transfer to the dimer may prevail.

## Introduction

Interaction of ultraviolet light with DNA leads to the formation of *cis*,*syn*-cyclobutane thymine dimers.[1,2] These lesions are known to be repaired by DNA photolyase, an enzyme which accommodates two photoreactive components: reduced flavin adenine dinucleotide, $FADH^-$, and 5,10-methenyltetrahydrofolylpolyglutamate (MTHF).[3] The crudely understood sequence of events during the repair process involves five steps:[1,2] (i) recognition of a DNA dimer defect by photolyase and structure specific binding, (ii) excitation of the photoreactive cofactor $FADH^-$, either directly or via excitation energy transfer from the cofactor MTHF, (iii) electron transfer from excited $FADH^-$ to the dimer, (iv) splitting of the cyclobutane bridge and back transfer of the electron, and finally (v) desorption of the enzyme from the repaired DNA substrate.

The crystal structure of DNA photolyase enzyme[3,4] shows an interesting feature of the proposed substrate binding site: a hole in the enzyme surface leads to the photoreactive component $FADH^-$ at the bottom of the pocket. $FADH^-$ is bound inside the enzyme; nevertheless, part of the chromophore is accessible to the solvent through the hole. The dimension of this pocket seems to be optimally suited to allow access of a DNA lesion to the cofactor, enabling the electron transfer that initiates the dimer splitting. Two significant exposed regions, a hydrogen bonded polar network and a hydrophobic shell, line the pocket. Both regions are expected to play an important role in the recognition and binding of a DNA dimer defect through steric and electrostatic interactions with the docking substrate. One may assume that the hydrogen bonded network favors the interaction with negatively charged phosphate groups of the DNA, while the neutral pyrimidine dimer is oriented toward the hydrophobic shell.

In a previous molecular dynamics (MD) study we characterized the chromophore $FADH^-$ and its binding to the enzyme.[5] The present work extends this MD work to elucidate the binding of selected model pyrimidine dimers to photolyase. Pyrimidine (Pyr) model dimers, like *cis*,*syn*-dPyr⟨p⟩dPyr, play an important role in elucidating details of the splitting reaction.[6,7] The designation of this model dimer indicates the link formed by desoxyribose (d) and phosphate (p) groups, Figure 1. In this work, we shall examine the "bare" dimer *cis*,*syn*-U⟨⟩T with both pyrimidine units linked only by a cyclobutane ring (U, uracil; T, thymine; Figure 1). To evaluate the influence of a DNA backbone fragment on the dimer docking the corresponding dimer *cis*,*syn*-dU⟨p⟩dT was also considered. Recently, a molecular modeling study based on slightly larger pyrimidine dimer models has been carried out in order to construct a model for the enzyme−substrate complex in question;[8] we shall also discuss similarities and differences compared to the present investigation.

In the following discussion we will focus exclusively on the cis,syn form, which is the one active in the DNA photo repair process. Therefore, we shall drop the qualifier "cis,syn" for convenience. The backbone fragment consists of a negatively charged phosphate moiety and two ribose groups. Furthermore, to broaden the scope of the present work we will discuss effects of the environment on the structure of the dimers by studying them in the gas phase as well as in aqueous solution.

## Computational Methods

The geometry optimization and molecular dynamic simulation procedures were performed by using the AMBER force field as provided by the program Discover, version 95.0.[9,10]

The crystal structure of photolyase including cofactors and crystal water molecules was chosen as initial geometry (Protein Data Bank entry: 1dnp).[3] To take solvent effects into account a sphere of 20-Å radius, centered at the entrance of the enzyme pocket, was filled with additional 516 water molecules. In this way the pocket is filled, the surface of the enzyme in the vicinity of the pocket is solvated, and the dimer is surrounded by water.

* Corresponding author.
[†] Present address: Institut für Angewandte und Theoretische Physik, Universität Stuttgart, 70550 Stuttgart,Germany.

10.1021/jp984197h CCC: $18.00 
Published on Web 03/03/1999

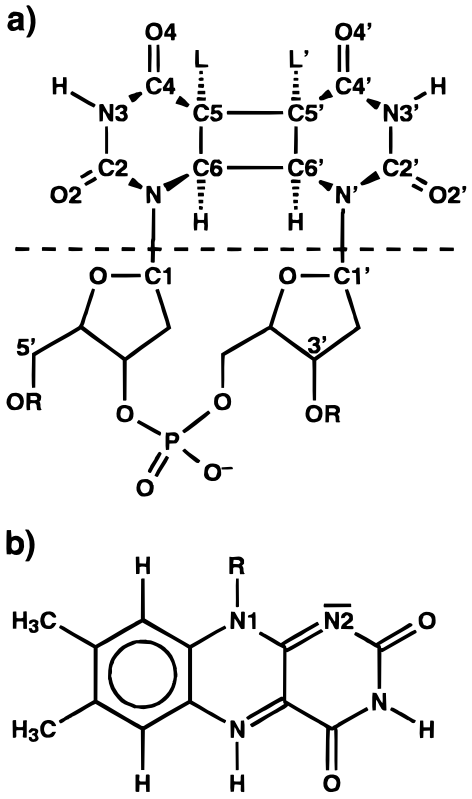


**Figure 1.** (a) Labeling scheme of model pyrimidine dimers. The bare dimer U⟨⟩T (L = $CH_3$, L′ = H) comprises the parts above the dashed line, with the bonds of N and N′ terminated by H atoms. The dimer dU⟨p⟩dT (L = $CH_3$, L′ = H) bearing ribose and phosphate moieties shown below the dashed line is terminated by R = H. (b) Labeling scheme of the isoalloxazine moiety of $FADH^-$; the substituent R indicates the remainder of the FAD molecule.

Unless otherwise mentioned, the water molecules and the protein were allowed to move freely during the simulation. Likewise, solvation of the model dimers was studied by immersing them in a shell of 20-Å radius filled with water molecules.

The potential types for the photolyase enzyme and the water molecules were chosen in standard fashion;[12−14] the charges of glutamic and aspartic acid are negative, while arginine and lysine are positively charged. The potential types and partial charges for $FADH^-$ have been described previously.[6] The partial charges of the dimers have been estimated by the semiempirical quantum chemistry method PM3 (which had been also used in the case of FAD[6]) as obtained with the program MOPAC 6.0.[11,12] Comparisons with semiempirical AM1 and density functional calculations yielded very similar results for the partial charges.[13,14] For the bare dimer U⟨⟩T the potential types and partial charges are assigned as specified in the following. First, the atom labels (see Figure 1), then the potential types (following AMBER conventions), and finally the partial charges are given: N/N/−0.584, H1/H/0.274, C2/C/0.886, N3/NA/−0.792, H3/H/0.282, C4/C/0.842, C5/CT/−0.095, C1/CT/−0.198, H11/HC/0.066, H12/HC/0.066, H13/HC/0.066, C6/CT/0.105, H6/HC/ 0.066, O2/O/−0.492, O4/O/−0.492, N′/N/−0.584, H1′/H/0.274, C2′/C/0.886, N3′/NA/−0.792, H3′/H/0.282, C4′/C/0.842, C5′/CT/−0.161, H5′/HC/0.066, C6′/CT/0.105, H6′/HC/0.066, O2′/O/−0.492, O4′/O/−0.492. The parameters for the other bare model dimers investigated in this study were chosen similarly. For the dimer model dU⟨p⟩dT linked to phosphate and ribose groups, the parameters of the base pair are (the overall charge of the dimer is −1 au) as follows: N/N/−0.319, C2/C/0.431, N3/NA/−0.370, H3/H/0.269, C4/C/0.324, C5/CT/−0.156, C1/CT/ 0.149, H11/HC/0.066, H12/HC/0.066, H13/HC/0.066, C6/CT/−0.174, H6/HC/0.136, O2/O/−0.382, O4/O/−0.320, N1/N/−0.306, C2′/C/0.431, N3′/NA/−0.370, H3′/H/0.263, C4′/C/0.315, C5′/CT/−0.158, H5′/HC/0.148, C6′/CT/0.029, H6′/HC/0.142, O2′/O/−0.356, O4′/O/−0.336. The parameters of the bonded ribose and phosphate groups are as follows: O5′/OH/−0.343, H5′/HO/0.215, O3′/OS/−0.726, C1′/CS/0.183, H1′/HT/0.145, C2′/CS/−0.243, H2′1/HT/0.147, H2′2/ HT/0.094, C3′/CS/0.054, H3′/HT/0.135, C4′/CS/−0.024, H4′/HT/0.125, C5′/CT/−0.016, H5′1/HC/0.060, H5′2/HC/0.111, O4′/OE/−0.310, P/P/2.529, O1P/O2/−1.148, O2P/O2/−1.154, O5′/OS/−0.753, O3′/OT/−0.333, HO3′/HY/0.217, C1′/CS/0.166, H1′/HT/0.127, C2′/ CS/−0.215, H2′1/HT/0.114, H2′2/HT/0.093, C3′/CS/0.003, H3′/HT/0.118, C4′/CS/−0.011, H4′/HT/0.083, C5′/CT/0.060, H5′1/HC/0.083, H5′2/HC/0.088, O4′/OE/−0.262.

For the nonbonded van der Waals interactions an atom-based cutoff at 9.5 Å was imposed. Long-range Coulomb interactions were evaluated with the cell multipole method.[15,16] Energy minimizations were performed using steepest descent and conjugated gradient methods[17] until the norm of the gradients was at most 0.01 kcal/mol/Å per atom. MD runs of the free dimer were executed at a temperature of 800 K in order to efficiently explore the conformation space, while for the dimer in water solvent as well as for the enzyme simulation the temperature was set to 300 K. In the case of free dimers and the dimers in aqueous solution, each MD run was carried out up to 150 ps with time steps of 1 fs. During the first 50 ps the system was equilibrated, the remaining simulation time was used for two independent samplings of 50 ps each and coordinates were saved every 0.5 ps. To equilibrate the photolyase enzyme a MD run up to 300 ps with 12 independent samplings was performed: one sampling of 80 ps followed by 11 independent samplings, 20 ps each. The resulting enzyme geometry was used as starting structure for the docking simulations. For the dimer docking of U⟨⟩T and dU⟨p⟩dT into photolyase, each simulation was performed up to 300 ps (15 independent samplings, 20 ps each). The dimer was located 25 Å from the bottom of the pocket. For each model dimer the 300 ps simulation period is split into the following sequence of subperiods of three different types. The first MD ran up to 180 ps and was related to the docking and binding situation of the dimer in the enzyme. Next, two simulation runs of two times 20 ps were performed to investigate the docking with different starting geometries of the dimer. These intervals of 20 ps were chosen after finding that this is the maximum time span it takes for the dimers to approach the enzyme pocket due to the attractive interactions. Thus, three independent docking simulations can be analyzed by this approach just described. Finally, to conclude the 300 ps simulation, the dependence of the dimer docking on another form of the reduced state of the chromophore was explored; $FADH_2$ instead of $FADH^-$ has been applied, again for a simulation period of two times 20 ps. The dihydro form $FADH_2$ is chosen to investigate the influence of the charge of the chromophore on the dimer docking. The structure of the enzyme and the distribution of the water molecules were carried on from each of the subperiod simulation to the next one, while the dimer or chromophore geometries were always "restarted" after each subperiod of two times 20 ps. During the simulations we checked carefully that the dimer was surrounded by water molecules.

The rendering of the three-dimensional structures displayed in the figures was carried out by using the program Schakal, version 97.[18]

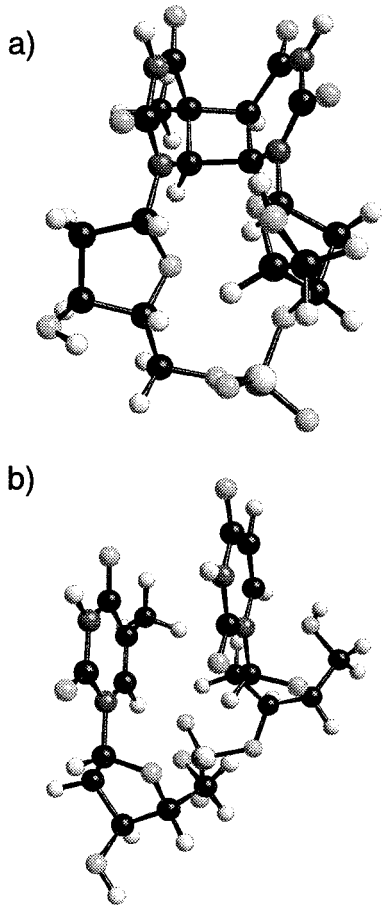


**Figure 2.** Representation of the model pyrimidine dimer dU⟨p⟩dT as optimized by AMBER (a) and a DNA backbone fragment carrying a uracil and a thymine base (b).

## Results and Discussion

**Structural Characteristics of Model Dimers.** MD simulations of model dimers in the gas phase and in water have been carried out to explore the conformational space of the dimers. Here, we analyze structures of the model dimers U⟨⟩T and dU⟨p⟩dT.

In general, the equilibrium structure of the model dimers are quite similar. They hardly change when going from the gas phase to an aqueous environment. As an example, we discuss the geometry of the bare dimer U⟨⟩T in some detail. The C−C bond lengths vary between 1.53 and 1.54 Å, and the C−O bond distances are 1.22 Å. The nitrogen to carbon bond lengths N3−C2 and N3−C4 are 1.37 Å (for the labeling see Figure 1), while somewhat different values, 1.33 and 1.46 Å, are calculated for N−C2 and N−C6, respectively. The various valence angles in the cyclobutane ring vary between 89 and 91°, and the bond angles of the six-membered pyrimidine rings are 114−119° in case of X−C−X (X = C, N) and 125−126° for X−N−X. Among the various dimers, bond lengths differ by less than 0.01 Å and bond angles by at most 3°.

The calculations yield a puckered structure for the four-membered cyclobutane ring. In the case of the bare dimer the dihedral angle C6−C5−C5′−C6′ is 11−12°, while for dU⟨p⟩dT the angle increases to 20° indicating that the ribose and phosphate groups apply some strain to the arrangement of the pyrimidine moieties. However, the ribose and phosphate groups do not significantly influence the arrangement of both pyrimidine moieties when compared to the bare dimer (see Figure 2a). Additional calculations on the dimers T⟨⟩U, U⟨⟩U, T⟨⟩T, and dU⟨p⟩dU yielded similar results; therefore we refrain from discussing them further. Experimental investigations and quantum chemical calculations on pyrimidine dimers yield somewhat larger dihedral angles C6−C5−C5′−C6′. The crystal structures of the uracil dimer[19] U⟨⟩T and the dimethylthymine dimer[20] exhibit dihedral angles of 25° and 27°, respectively, while quantum chemical calculations on free dimers at the Hartree−Fock level yield dihedral angles of 20.5° for U⟨⟩U[21] and 17.9° for T⟨⟩T.[22] Thus, while the AMBER calculations underestimate the nonplanarity of the cyclobutane ring, the overall structure of the dimers are in satisfactory agreement with experiment and quantum chemical calculations on similar model dimers.[17,18,24−23]

As expected, the computational results of the equilibrium structures show that the main differences between the distinct dimers are due to steric interactions which are connected to structural features, e.g., (i) whether a methyl group is present (in case of thymine) or not (in case of uracil) or (ii) whether the ribose and phosphate groups are bonded to the pyrimidine dimer (in case of dU⟨p⟩dT) or not (in case of U⟨⟩T). No further significant differences between the distinct model dimers were found.

Next, we turn to a discussion of the MD results. The geometries of the free dimers and the dimers in a water solvent vary slightly from the corresponding equilibrium structures: the mean bond lengths and valence angles deviate from the equilibrium structure by less than 0.01 Å and 3°, respectively. The maximum standard deviations are 0.04 Å for the bond lengths, 4° for the valence angle X−C−X, and 10° for X−N−X. The distances between nonbonded atoms are subject to somewhat larger variations. For example, it is of interest to investigate the mobility of both pyrimidine rings against each other. The rings are linked by chemical bonds C5−C5′ and C6−C6′, while essentially nonbonded interactions occur between the atoms C2−C2′ and N3−N3′. The mean value of both nonbonded distances is about 3.6 Å for each model dimer, just as for the equilibrium structures. However, the standard deviations calculated during the MD runs for both nonbonding distances are up to almost 0.2 Å in case of the dimer surrounded by solvent water but up to almost 0.4 Å in the free dimers. Note that the latter simulations exhibiting larger standard deviations were performed at an elevated temperature of 800 K (usually 300 K is used). However, these "high temperature" simulations of the free dimers did not reveal any other conformations. Interestingly, the dihedral angles C6−C5−C5′−C6′ for each model dimer (in the gas phase and in water solvent) are about 13−14°. The standard deviations are 6° for a dimer solvated in water and 10° for the "high temperature" free dimer simulations.

In conclusion, the dimers under investigation are conformationally rather inflexible. The overall structures are independent of the molecular environment: free dimers and dimers solvated in water exhibit quite similar geometries. Also, in the MD simulations of the dimer docking (see below) no significant change in the dimer structure has been found. Therefore, it is meaningful to employ model dimers for studying the influence of a methyl group bonded to C5 or C5′ as well as of the DNA backbone fragment on the docking of the enzyme to a DNA lesion. It is worth mentioning that after the repair of a DNA lesion the dimer bearing moiety of the ribose and phosphate groups becomes conformationally flexible due to possible rotations around the backbone bonds of the phosphate group (see Figure 2b). This results in structures with significantly larger steric demand than in the case of a pyrimidine dimer; in turn,

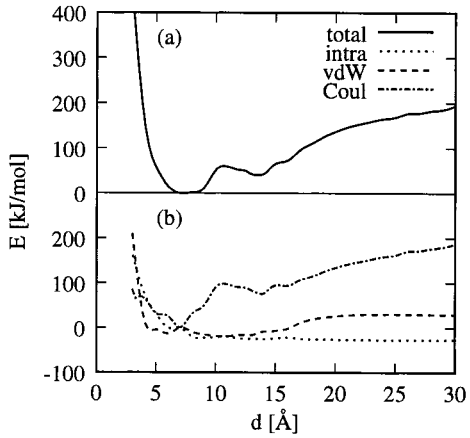


**Figure 3.** Static shape of the enzyme pocket as characterized by the minimum interaction energy *E* (in kJ/mol) between the enzyme and a probe dimer U⟨⟩T at a fixed distance *d* (for details, see the text). (a) Energy change as a function of the dimer distance *d* above the bottom of the pocket. (b) Changes of the van der Waals, Coulomb, and intradimer energy contributions. All energies have been normalized to their value at $d = 6$ Å, i.e., to the value at close contact between the probe and the chromophore at the bottom of the pocket.

one can assume that repaired structures will no longer fit into the enzyme pocket and thus will be expelled from the enzyme.

**Characterization of the Enzyme Pocket.** Before discussing the docking of a model dimer into the enzyme, we will analyze the binding site, i.e., the shape of the enzyme pocket.

We start by focusing on the "static" shape of the pocket. For this purpose, we applied the following procedure: (i) the enzyme and the atoms of FAD were fixed in their locations as determined in the crystal structure,[3] (ii) all crystal water molecules were removed from the pocket, (iii) the distance *d* between a probe model dimer U⟨⟩T and the bottom of the pocket was reduced step by step from 30 to 3 Å, and (iv) at each step the energy was minimized by allowing all internal degrees of freedom of the probe dimer to relax and its relative orientation to vary inside the enzyme pocket. The distance *d* is measured from the N1 center of FAD and the O4 atom of the probe (see Figure 1). Thus, the calculated energies are expected to provide a crude characterization for the shape of the enzyme pocket (see Figures 3 and 4). The energy is normalized to zero at a distance of $d = 6$ Å for which the lowest energy is found. This distance corresponds to a close contact between the probe dimer and the chromophore at the bottom of the enzyme pocket.

The simulations show that the interaction between the probe and the enzyme is attractive. The initial attraction acting on the probe dimer leads to a low-energy region at about $d = 12-14$ Å above the bottom of the pocket (Figure 3a). We shall refer to this region where the pocket opens toward the surface as the "pocket entrance" region. Further reduction of distance *d* leads to an energy barrier of about 18 kJ/mol above this first minimum configuration at a distance of 11 Å (Figure 3a). In the following, we shall refer to this region with distances *d* from 8 to 12 Å as "bottleneck" of the enzyme pocket. A second minimum arrangement is found at close van der Waals contact between the probe dimer and the chromophore at the bottom of the pocket ($d = 6$ Å; see Figure 3a). It is interesting to analyze how the overall energy (change) *E* of the dimer−enzyme system is formed from the changes of various contributions during the docking procedure (see Figure 3b). From distances *d* of about 30 Å down to 8 Å, the probe dimer exhibits a relaxed structure as indicated by the low values of the intramolecular energy, while at close contact this intramolecular energy increases by about 19 kJ/mol relative to the relaxed dimer energy. This latter

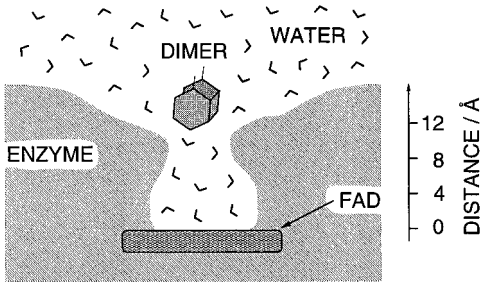


**Figure 4.** Schematic view of the pocket in the enzyme: $FADH^-$ at the bottom of the pocket; water molecules and a bare dimer at the entrance region. The "antennas" indicate the linking atoms to the ribose and phosphate backbone atoms. At a distance of 8−12 Å above the bottom of the pocket a bottleneck region is indicated, and for *d* in the range 12−14 Å, the pocket entrance region is shown, which opens toward the enzyme surface.

change indicates that the enzyme affects the dimer structure to some extent. However, the main contribution to the total energy change E as shown in Figure 3 arises from the dimer-to-enzyme nonbonding interaction. The van der Waals contribution decreases steadily with distance *d*, down to the close contact between the dimer and the chromophore, thus contributing substantially to the attractive interaction between the dimer and the enzyme. On the other hand, the Coulomb interaction changes noticeably with distance *d* and determines the overall energy change within the enzyme pocket to a significant degree. During the dimer approach the Coulomb contribution is attractive; it shows two low energy regions at 12−14 Å and at about 6 Å separated by a barrier in the range from 8 to 12 Å (which is the bottleneck). Essentially the same shape characteristics of the enzyme pocket were found in other simulations where different atom centers were used to measure the distance from FAD to the dimer or where other bare dimer probes were employed. One expects that relaxation of the enzyme will open the bottleneck to some extent. However, MD simulations to be described below do not confirm this hypothesis. In Figure 4 a schematic view of the enzyme pocket is sketched, summarizing the results of the static calculations as well as of the dynamic simulations to be discussed below. Considering the bulky shape of the dimer dU⟨p⟩dT, one can expect this bottleneck to considerably restrict the penetration depth of such linked dimers.

The "dynamic" shape of the pocket has been investigated by MD simulations taking into account the enzyme, the chromophores, and the crystal as well as solvent water molecules. The system (without the dimer) was simulated for a period of 300 ps (see the section Computational Methods). The MD simulation shows little variation of the overall enzyme structure relative to that determined by the X-ray analysis. The RMS values of the enzyme backbone atoms are $2.0 \pm 0.3$ Å in the time window from 80 to 300 ps. Although the amino acids are quite mobile two specific regions of the pocket found in the crystal structure (as described in the Introduction) persist, (i) the hydrogen bonded network and (ii) the hydrophobic shell. Both regions constitute a substantial part of the enzyme pocket surface region in which the contact between the dimer and the electron donor FAD will take place. Moreover, the chromophore $FADH^-$ remains located at the bottom of the pocket and is "covered" in part by amino acids of both characteristic regions (for details see ref 6). However, part of the photoactive center of $FADH^-$ is accessible to water molecules and to the substrate. During the MD simulation an average of about 19 water molecules is found inside the pocket within a 10-Å distance measured from the nitrogen center N1 of FAD toward the enzyme surface. (This corresponds to the region between the

bottom of the pocket and the location of the bottleneck at $d = 6$ Å.) Within a distance of 15 Å from N1 one finds 59 water molecules. The standard deviations of these quantities amount to about three and six water molecules, respectively.

To further investigate the shape of the pocket, the RMS value of the backbone atoms of the amino acids which form the pocket has been calculated. The amino acids were selected in the following manner. At a distance of 10 Å from the nitrogen atom N1 of FAD, which links the isoalloxazine and ribose units, in the direction toward the entrance of the pocket two concentric spheres have been located; the radii, 8 and 10 Å, are applied. According to this criterion, the following amino acids are taken into account for a radius of 8 Å: Arg226, Asp227, Asn273, Glu274, Trp277, Asn341, Arg342, Met345, Trp384, Phe399. In case of a radius of 10 Å the additional amino acids are Phe150, Lys154, Tyr222, Glu223, Val270, Tyr281, Gly381, Asp391, Ala392, Ala393, Arg397, and Phe408. In this way, the MD simulation leads to RMS values of 1.5 ± 0.2 Å (radius 8 Å) and 1.6 ± 0.2 Å (10 Å). This implies that the pocket does not exhibit large structural changes compared to the enzyme as a whole, since both RMS values are somewhat smaller than the RMS value of the enzyme backbone atoms (2.0 ± 0.3 Å).

No significant changes in the shape of the pocket as well as of structure and location of the chromophore have been found during the simulations. Therefore, as far as MD simulations are concerned, the dimer docking procedure is expected to be dominated by steric and electrostatic interactions between the dimer, solvent water molecules, and the enzyme; conformational rearrangements of the enzyme, which might strongly influence the docking, do not seem to be of major importance.

**Dimer Docking to Photolyase.** The MD simulations were performed on a system composed of photolyase, the chromophore $FADH^-$, a model dimer (either U⟨⟩T or dU⟨p⟩dT), and solvent water molecules filling the pocket as well as solvating the enzyme and the dimer. The docking simulations were started from relaxed enzyme and water solvent geometries (see the section on Computational Methods). At the start of the MD simulations, the dimer was located at a distance of 25 Å from the bottom of the enzyme pocket.

During the simulations the dimer geometries are rather similar to those of free dimers and of dimers in water which were discussed above. No significant influence of the photolyase enzyme on the model dimer structures was found. For example, the nonbonding distances C2−C2′ and N3−N3′ remain at about 3.6 ± 0.2 Å in each case, and the dihedral angle of the cyclobutane ring atoms is 10 ± 8° for the bare dimer and 14 ± 7° in case of dU⟨p⟩dT.

As already mentioned above, the docking of the dimer into the enzyme was modeled in three independent MD runs for each dimer. For the following subperiod of 20 ps each dimer is "observed" inside the pocket. A typical snapshot of the bare dimer inside the pocket is displayed in Figure 5. Similar results were found for simulations where another possible form of the reduced state of the chromophore, $FADH_2$ instead of $FADH^-$, was considered. One MD run of two times 20 ps time for each model dimer was performed. The second form of the reduced state showed very similar behavior during the docking simulations. As before, the dimer model approaches the pocket during the first 20 ps. However, one has to take into account the charge distribution of $FADH^-$, which is assumed to be the same in the enzyme and in the gas phase. With the given binding to the enzyme, this implies that the negative charge density is directed toward the interior of the protein, i.e., away from the approaching dimer.[6] Therefore, this charge is not at all exposed to the solvent and the substrate in the enzyme pocket. Whether such a charge distribution holds also "in vivo" is not known as the present calculations do not account for the charge distribution in the electronically excited-state $FADH^{-*}$ nor do they include any charge modification of the chromophore under the influence of the protein environment or of the molecules in the enzyme pocket (water and substrate).

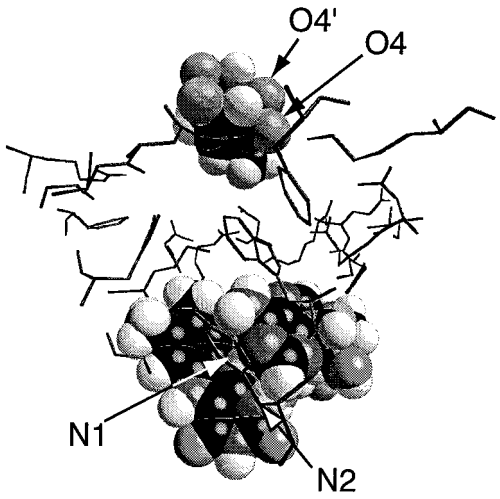


**Figure 5.** Snapshot of the dimer docking process as calculated by the MD simulation. The model dimer U⟨⟩T, $FADH^-$ bound in the enzyme, and several amino acid groups adjacent to the dimer and to $FADH^-$ are shown. Hydrogen atoms of the amino acids are omitted for clarity. In the figure, the enzyme pocket containing the model dimer extends upward. The protein surrounds the chromophore in all other directions; isoalloxazine, the photoactive moiety of $FADH^-$, is in part directed toward the interior of the enzyme (downward in the figure).

To investigate the binding geometry of the dimers in the pocket one of the above-mentioned MD simulations was continued up to 180 ps for each model dimer. In the MD runs for the bare dimer all the atoms (and all amino acids) were allowed to move freely during these simulations, while for dU⟨p⟩dT all amino acids except the ones forming the pocket and the pocket entrance region were fixed in their position after 40-ps simulation time; following the PDB labeling scheme the fixed amino acids are 1−127, 166−193, and 419−469. In all cases the dimers remained in the enzyme pocket from 20 to 180 ps.

Before discussing the binding of the dimer, we shall characterize the enzyme and its pocket. The RMS values of all enzyme backbone atoms in the time window from 20 to 180 ps are 2.6 ± 0.7 Å for the docking of U⟨⟩T; a value which is larger than during the preceding relaxation of the enzyme alone. For dU⟨p⟩dT the RMS of all enzyme backbone atoms was calculated as 1.9 ± 0.4 Å in the time window from 20 to 40 ps. The RMS values of the enzyme pocket atoms are somewhat smaller than or at most equal to the RMS values of all backbone atoms. For U⟨⟩T these values are 2.4 ± 0.8 and 2.6 ± 0.7 Å for selected radii (see above) of 8 and 10 Å, respectively. Both values indicate that the pocket backbone atoms are as mobile as the atoms of the whole enzyme. In case of dU⟨p⟩dT the RMS values of the pocket backbone atoms have been calculated for a time window of 20 to 40 ps: 1.0 ± 0.2 Å (8 Å) and 1.5 ± 0.3 Å (10 Å). These smaller values seem to be a consequence of our model strategy (see above): fixing distant amino acids apparently reduces the flexibility of the pocket atoms.

As expected, the penetration depth of the model dimer is limited by steric interactions between the dimer and the enzyme, especially in the bottleneck region of the pocket entrance, as well as by the solvent water molecules inside the pocket. In Figure 6 the minimum van der Waals distance between the dimer

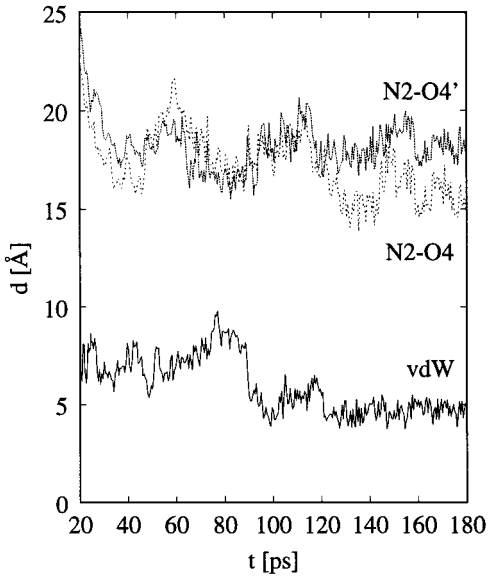


**Figure 6.** Minimum van der Waals distance *d* between the dimer U⟨⟩T and the $FADH^-$ molecule at the bottom of the pocket as a function of the simulation time *t*. Also shown are the distances between the nitrogen center N2 of $FADH^-$ and the oxygen centers O4 and O4′ of the dimer U⟨⟩T.

U⟨⟩T and the $FADH^-$ molecule is plotted against the simulation time. During the time window from 20 to 80 ps the mean distance is about 7 Å and for 100 to 180 ps it is reduced to about 5 Å. Compared to the "static" simulation results where no water molecules were admitted inside the pocket and the dimer gets in close contact to the chromophore $FADH^-$, one finds in the present MD calculations the minimum van der Waals distance of the dimer from the bottom of the pocket to be enlarged by about 5 Å. The minimum distance between the center N2 of the electron donor FAD and the center O4 of the electron accepting dimer is about 15 Å (see Figure 6).

The water molecules around the entrance region of the pocket are quite easily pushed away by the substrate: about eight solvent molecules (of 59) are removed by an approaching dimer U⟨⟩T from the larger sphere of 15-Å radius measured from center N1 of FAD. A bare dimer displaces the same number of eight solvent molecules when placed in a water solution. As a result, the bare dimer is fully drawn into the pocket entrance region. A significant number of water molecules remain inside the pocket even with the substrate dimer present. As mentioned in the section concerning the characterization of the enzyme pocket, about 19 water solvent molecules reside on the average inside the enzyme pocket proper (behind the bottleneck), prior to a dimer being present inside the enzyme pocket. With U⟨⟩T in the pocket, 15 solvent molecules are still found within a radius of 10 Å from the center N1 of FAD. Thus, speaking figuratively, the dimer is located at the bottleneck similar to a stopper on a bottle. However, no direct contact between the dimer and the chromophore occurs, a result that is in accordance with another recent MD study on the docking of a similar dimer model.[11] This is also true for the other dimers under investigation. Additional MD simulations have been performed to study the docking of the bare dimer T⟨⟩U, leading to a similar minimum van der Waals distance of about 7 Å. The distance between the centers N2 of FAD and O4 of the dimer is larger than 17 Å. Thus, for bare dimer T⟨⟩U the MD simulations yield a slightly larger distance between donor and acceptor of the electron transfer than for U⟨⟩T, paralleling the electron-transfer rate, which has been measured to be faster for U⟨⟩T than for T⟨⟩U.[7] In the context of electron transfer, it is interesting to note that the center N2 of the donor $FADH^-$ is directed toward the interior of the enzyme. This feature might imply that indirect electron transfer from the flavin cofactor to the pyrimidine dimer may prevail, e.g., via Trp277 or Trp384. Both tryptophans have been shown to be important for DNA binding.[24,25] This line of argument holds even more for the dimer dU⟨p⟩dT where the minimum van der Waals distance is larger than 9 Å and the distance from the center N2 of FAD to the center O4 of the dimer is larger than 19 Å.

We note that all dimers are rather mobile in the pocket region. To quantify the mobility, the distance per given time interval of the center of mass of the pyrimidine rings has been determined. On the average, U⟨⟩T moves by about 1.0 ± 0.6 Å/ps and dU⟨p⟩dT by 1.6 ± 0.6 Å/ps. The bare dimer is somewhat less mobile than dU⟨p⟩dT; this difference is likely due to the fact that the former penetrates deeper into the enzyme pocket. No indication of an orientational preference of the bare dimer is found. In case of the dimer bearing ribose and phosphate groups the pyrimidine moieties are directed toward the enzyme pocket, while the bulky backbone fragment restricts the penetration depth due to its interaction with the amino acids forming the pocket entrance region.

All miminum distances of the dimers from the bottom of the pocket as determined in the MD simulations are significantly larger than those obtained in the "static" simulation described previously, for which a close contact between the chromophore and the dimer was found. These latter values refer to situations where no water molecules were present which otherwise prevent any direct contact between the chromophore FAD and the dimer. For the bulky dimer dU⟨p⟩dT, already the steric interactions of the phosphate and ribose backbone fragment with the enzyme precludes any closer contacts. Bare dimers apparently advance about 4 Å more into the pocket.

While the present MD simulations may not be large enough to explore the full phase space of these complex systems it is satisfactory to note the general agreement of our results with those of a similar study that was carried out independently.[11] There, a slightly larger dimer model with additional phosphate units, p-dU⟨p⟩dT-p, and a single stranded DNA nonamer containing a pyrimidine dimer moiety has been used. That study focuses on Coulomb interactions of the dimer with residues near the active site rather than on quantitative distance criteria as in the present work. Also, the role of crystal and additional solvent water was not considered in detail. Nevertheless, taking into account the observed rates of electron transfer[7] and the large distance from the FADH cofactor to the dimer, an indirect transfer path has been suggested as well.[11]

## Conclusions

We have carried out MD simulations on the docking of photolyase to a photoinduced pyrimidine dimer defect of DNA. Our discussion focused (i) on the flexibility of the pyrimidine model dimers, (ii) on the shape of the enzyme pocket, and (iii) on the docking and binding of the dimer to this pocket. In summary, we find the following:

(i) A conformational analysis of the model dimers in different environments (in the gas phase, in water solution, and in the enzyme−substrate complex) reveals that these dimers are essentially inflexible and that various pyrimidine dimer models exhibit similar overall shapes. This results is as expected from a chemical point of view. Two types of models have been considered in detail: bare dimer U⟨⟩T and the more extended dimer model dU⟨p⟩dT linked by a bulky backbone fragment (ribose−phosphate−ribose, Figure 1).

(ii) The shape of the pocket has been investigated by "static" and "dynamic" simulations. The former have been performed by removing the water molecules and keeping the enzyme atoms fixed in their crystal positions while the distance between a probe molecule and the bottom of the pocket was reduced step by step. A bottleneck region is identified at about 8−12 Å above the bottom of the pocket (where the chromophore $FADH^-$ is located) in the direction toward the surface of the enzyme. At larger distances the pocket opens toward the enzyme surface. The MD simulations of the enzyme including the water molecule demonstrate that the shape of the pocket in the enzyme resembles the one determined in the crystal structure analysis.[3]

(iii) Attractive interactions (both van der Waals and Coulomb interactions) lead to the docking of the dimer into the enzyme pocket. As expected, the dimension of the pocket is well suited for receiving pyrimidine dimers. The penetration depth depends on the model type. For the bare dimer U⟨⟩T a minimum van der Waals distance of 5 Å between the bottom of the pocket and the dimer is found; about 15 water molecules fill the space between the pocket bottom and the dimer. The minimum distance between the center N2 of FAD and the center O4 of the dimer is about 15 Å. In the case of the bulky dimer dU-⟨p⟩dT steric interactions between the backbone and the bottleneck as well as with the pocket entrance region limit the van der Waals distance between the chromophore FAD and the dimer to about 9 Å; the closest distance from the N2 center of FAD to the O4 center of the dimer is at least 19 Å. No direct contact between the model dimers and the photoactive $FADH^-$ molecule was found. All these findings taken together make a direct electron transfer from FAD to the dimer unlikely,[11,26] in particular since the DNA backbone may lead to even larger donor−acceptor distances than those found in the present study for the model dimers.

**Acknowledgment.** We are grateful to J. Rak and A. A. Voityuk for helpful discussions and for carrying out the AM1 and DF calculations on the bare dimers. We also thank O. G. Wiest for communicating his work prior to publication. This work has been supported by the Deutsche Forschungsgemeinschaft (SFB 377 and GRK 285) and the Fonds der Chemischen Industrie.

## References and Notes

(1) Sancar, A. In *Advances in Electron-Transfer Chemistry*; Mariano, P. E., Ed.; JAI Press: London, 1992; Vol. 2, p 215.
(2) Rose, S. D. In *CRC Handbook of Organic Photochemistry and Photobiology*; Horspool, W. M., Ed.; CRC Press: New York, 1995; p 1332.
(3) Park, H.-W.; Kim, S.-T.; Sancar, A.; Deisenhofer, J. *Science* **1995**, *268*, 1866.
(4) Sancar, A. *Biochemistry* **1994**, *33*, 2.
(5) Heelis, P. F.; Hartman, R. F.; Rose, S. D. *J. Photochem. Photobiol. A Chem.* **1996**, *95*, 89.
(6) Hahn, J.; Michel-Beyerle, M.-E.; Rösch, N. *J. Mol. Med.* **1998**, *4*, 73.
(7) Langenbacher, T.; Zhao, X.; Bieser, G.; Heelis, P. F.; Sancar, A.; Michel-Beyerle, M.-E. *J. Am. Chem. Soc.* **1997**, *119*, 10532.
(8) Kim, S.-T.; Sancar, A. *Biochemistry* **1991**, *30*, 8623.
(9) Zhao, X.; Sancar, A.; Heelis, PF.; Langenbacher, T.; Heinecke, R.; Musewald, C.; Kompa, C.; Pöllinger-Dammer, F.; Michel-Beyerle, M.-E. *Biophys. J.* **1997**, *72*, A137.
(10) Epple, R.; Wallenborn, E.-U.; Carrel, T. *J. Am. Chem. Soc.* **1997**, *119*, 7440.
(11) Sanders, D. B.; Wiest, O. G., unpublished.
(12) Weiner, S. J.; Kollmann, P. A.; Case, D. A.; Singh, U. C.; Ghio, C.; Alagona, G.; Profeta, S. J.; Weiner, P. *J. Am. Chem. Soc.* **1984**, *106*, 765.
(13) Weiner, S. J.; Kollmann, P. A.; Nguyen, D. T.; Case, D. A. *J. Comp. Chem.* **1986**, *7*, 230.
(14) *Discover User Guide*; Biosym/MSI: San Diego, 1995.
(15) Stewart, J. J. P. *MOPAC 6.0*; *Quantum Chemistry Program Exchange*, no. 455, 1990.
(16) Stewart, J. J. P. *J. Comp. Chem.* **1989**, *10*, 209, 221.
(17) Voityuk, A. A.; Michel-Beyerle, M.-E.; Rösch, N. *J. Am. Chem. Soc.* **1996**, *118*, 9750.
(18) Rak, J.; Voityuk, A. A.; Rösch, N., *J. Phys. Chem. A* **1998**, *102*, 7168.
(19) Greengard, L.; Rokhlin, V. I. *J. Comp. Phys.* **1987**, *73*, 325.
(20) Schmidt, K. E.; Lee, M. A. *J. Stat. Phys.* **1991**, *63*, 1223.
(21) Ding, H. Q.; Karasawa, N.; Goddard, W. A. *J.Chem. Phys.* **1992**, *97*, 4309.
(22) Press, W. H.; Teukolsky, S. A.; Vetterling, W. T.; Flannery, B. P. *Numerical Receipts*, 2nd ed.; Cambridge UP: Cambridge, 1992.
(23) Keller, E. *Schakal97*; Kristallographisches Institut der Universität Freiburg: Germany, 1997.
(24) Adman, E.; Gordon, M. P.; Jensen, E. H. *J. Chem. Soc., Chem. Commun.* **1968**, 1019.
(25) Camerman, N.; Camerman, A. *J. Am. Chem. Soc.* **1970**, *92*, 2523.
(26) Voityuk, A. A.; Rösch, N. *J. Phys. Chem. A* **1997**, *101*, 8335.
(27) Aida, M.; Kaneko, M.; Dupuis, M. *Int. J. Quantum Chem.* **1996**, *57*, 949.
(28) Aida, M.; Inoue, F.; Kaneko, M.; Dupuis, M. *J. Am. Chem. Soc.* **1997**, *119*, 12274.
(29) Li, Y. F.; Sancar, A. *Biochemistry* **1990**, *29*, 5698.
(30) Li, Y. F.; Heelis, P. F.; Sancar, A. *Biochemistry* **1991**, *30*, 6322.
(31) Kim, S. T.; Heelis, P. F.; Sancar, A. *Methods Enzymol.* **1995**, *258*, 319.